© Universiti Tun Hussein Onn Malaysia Publisher's Office

IJIE

http://penerbit.uthm.edu.my/ojs/index.php/ijie
ISSN : 2229-838X e-ISSN : 2600-7916

The International Journal of Integrated Engineering

Heat and Mass Transfer on MHD Flow Problems with Hall and Ion Slip Effects on Exponentially Accelerated Plate

Kamala Pratapa[1], Siva Reddy Sheri[2*]

[1]Department of Mathematics, CMRCET,
Kandlakoya, Medchal, Telangana, INDIA

[2]Department of Mathematics,
GITAM School of Science, Hyderabad Campus, Telangana, INDIA

[*]Corresponding Author

DOI: https://doi.org/10.30880/ijie.2023.15.05.015
Received 26 February 2023; Accepted 18 June 2023; Available online 19 October 2023

Abstract: We in this paper intended to investigate heat and mass transfer for MHD free convective flow for exponentially accelerated plate. The effects of Ion slip and Hall are studied considering variable temperatures, concentration, and angle of inclination. We applied finite element analysis for solving governing equations. Flow velocity, concentration and temperature's graphical profiles are examined for non-dimensional parameters. Flow reversal is prevented due to magnetic field, is observed. Velocity experiences retarding effect due to angle of inclination, this helps in acknowledging drag force in seepage flow.

Keywords: MHD, FEM, Hall and Ion Slip Effects, heat and mass transfer

1. Introduction

Simple flows are studied to understand the effects of porous medium. Flows in agriculture engineering, ground water drainage, natural gas, refining process have simple flows where effects on porous medium are studied theoretically and experimentally. Apart from existing knowledge about above engineering branches many more problems are significant, namely application of coriolis forces for application in rolled liquid. The rotating fluids play a very important role in atmospheric science, limnology, and meteorology. Viscous incompressible fluids in rotating frame have investigated HMD's. Fluid engineering has applications in rotating frames and has significance in geophysical and astrophysical sciences. The action of coriolis and magnetic forces governs turbo machines, MHD generator flow, Ekman pumping. Effects coriolis forces are more significant than viscous forces and inertial forces.

Veera Krishna [1] studied effects of ion-slip and Hall effects on MHD flows within gyratory frame. Mukhopadhyay [2] investigated unsteady convective flow for thermal radiation effects for stretching surface on porous medium. Ram [3] studied rotating free convective generating flows for ion slip and Hall currents. Seddeek [4] studied micro magneto polar fluids for ion slip, Hall effects and heat transfer. Bhatti et al. [5] studied peristaltic flow of blood in Eyring powell for permeable channel under "zero" Reynolds number for effects of ion slip and Hall currents. Uddin and Kumar [6] studied flows of boundary layer thickness of micro polar fluid and effects of ion slip and hall currents. Jitendra and Srinivasa [7] studied convective flow in rotating liquid for ion slip and Hall effects. Veera Krishna and Chamkha [8] studied hall current for MHD squeezing flow for Nano fluid which is water based in permeable medium between parallel disks. Veera Krishna and Chamkha [9] studied free convective MHD rotating Nano flows for porous plate under constant heat source. Veera Krishna et al. [10] studied effects of Hall for mixed convective flows, MHD's incompressible conducting viscous fluids, soret and joule effects are also considered. Mohamed et al. [11] studied pairs of diffusive flow in impermeable naturally convective fluids and placed in shortest sides rectangular inclined enclosure.

*Corresponding author: sreddy7@yahoo.co.in

Khilap et.al. [12] studied effect's chemical reaction for micro polar stagnation point flow MHD with slip and boundary conditions on convective flows over stretching sheet. Padam et al. [1]3 studied incompressible viscous, forced convective, Nano fluids in vicinity of magnetic field for heat transfer. Alok and Manoj [14] studied MHD Nano fluids past wedge in convective surfaces in porous medium for viscous dissipation and suction. Alok and Manoj [15] studied effects of heat transfer on Water-Cu Nano fluids on a stretching cylinder. Malvandi et al. [16] studied unsteady stagnation Nano fluids for slip effects on stretching sheet.

Satyanarayana et al. [17] studied Hall current and absorption of radiation in micro polar MHD fluid on rotating system. Sugunamma et al. [18] studied MHD radiation, heat mass transfer and chemical reaction for electrically conducting permeable plate under influence inclined magnetic field. Amos Emeka et al. [19] studied free convective flows which are MHD on inclined permeable medium for variable suction and effects of radiation. Makinde [20] studied permeable Nano fluids hydro magnetic boundary layer flows over moving surfaces. Hamad and Pop [21] studied Nano fluids of free convective nature past permeable flat plate with heat source which is constant. Kran Kumar et al. [22] studied mass and heat transfer in free convective flows in rotating frame through permeable medium for chemical reactions and thermo-diffusion. Khan [23] studied nonlinear thermal radiation and slip is understood by viscous fluid in a stretchable rotating disk. Devi et al. [24] studied Hall Effect and magnetic effect for radiation parameter for viscous MHD Newtonian fluid past rotating disk and electrically conducting fluid. Aziz and Afify [25] studied hall current on MHD slip on Nano fluid over stretching sheet. Siva Reddy Sheri and Anjan Kumar [26] studied mass and heat transfer over spontaneously moving vertical plate for furiously moving temperature. Siva Reddy Sheri et al. [27] studied natural convective flow for mass and heat transfer for MHD past infinite inclined plate.

Inspired by the above literature survey, we notified the need for analyzing effects of ion-slip and Hall on MHD not steady free convective flows over exponentially inclined accelerated plate. Hence filling the gap, we analyzed ion slip and Hall effect on inclined plate exponentially accelerating for permeable saturated substance carrier for free convective MHD rotating flow where angle of inclination, concentration and variable temperatures are considered.

2. Formulation of The Problem

We considered radiating fluid, which is not steady free convective MHD rotating, incompressible, viscous flows over exponentially slanted plate with differing temperatures in permeable saturated substance carrier with the influence of unvaryingly trans versing magnetic field which is of strength B_0 orthogonal to inclined plate. x-axis is parallel to the plate and z-axis orthogonal to plate. The angle of inclination is α. Induced magnetic field is not considered because of small Reynolds number. Initially the plate and fluid are in rotation with speed Ω. By assumption the plate and surrounding fluid are at concentration C_α and temperature T_α. The initial velocity for accelerated exponentially plate for $t > 0$ is $u = u_0 e^{a't}$, $v = 0$ at that instance temperature and concentration are lowered and raised. The boundary layer equations for the physical model for mass and heat transfer over accelerated exponentially slant plate is:

$$\frac{\partial u}{\partial x} = 0 \tag{1}$$

$$\frac{\partial u}{\partial t} - 2\Omega v - \nu\frac{\partial^2 u}{\partial z^2} - \frac{B_0 J_y}{\rho} + \frac{\nu}{k}u - g\beta(T - T_\infty)\cos\alpha - g\beta^*(C - C_\infty)\cos\alpha = 0 \tag{2}$$

$$\frac{\partial v}{\partial t} + 2\Omega u - \nu\frac{\partial^2 v}{\partial z^2} + \frac{B_0 J_x}{\rho} + \frac{\nu}{k}v = 0 \tag{3}$$

$$\frac{\partial T}{\partial t} - \frac{k_1}{\rho C_p}\frac{\partial^2 T}{\partial z^2} + \frac{S^*}{\rho C_p}(T - T_\infty) + \frac{1}{\rho C_p}\frac{\partial q_r}{\partial z} - \frac{1}{\rho C_p}\left(\frac{\partial u}{\partial z}\right)^2 = 0 \tag{4}$$

$$\frac{\partial C}{\partial t} - D\frac{\partial^2 C}{\partial z^2} + Kr^*(C - C_\infty) = 0 \tag{5}$$

The initial and boundary conditions are:

$$u = 0, v = 0, T = T_\infty, C = C_\infty, \forall\, z, t \le 0 \tag{6}$$

$$u = u_0 e^{a't}, v = 0 \;\; T = T_\infty + \frac{(T_w - T_\infty)tu_0^2}{\nu}, C = C_\infty + \frac{(C_w - C_\infty)tu_0^2}{\nu} \;\text{ as }\; z = 0 \tag{7}$$

$$u = v = 0, T \to T_\infty, C \to C_\infty \; as \; z \to \infty \tag{8}$$

Temperature boundary conditions are linear with time and with residual temperature T_∞ and with constant slope u_0^2/ν. The regional derivative for thin optical gas which is gray:

$$\frac{\partial q_r}{\partial z} = -4a^*\sigma((T_\infty^4 - T^4) \tag{9}$$

Similar to gray fluids absorbent /emitting fluids are considered but medium is not-scattering. By neglecting higher powers using Taylor series about T_∞ we consider:

$$T^4 \cong 4T_\infty^3 T - 3T_\infty^4 \quad (10)$$

The collision frequency of atom and electron is high hence ion slip and hall current cannot be neglected. By generalized ohm's law and including ion slip and Hall effect the influence of large magnetic field is:

$$J = \sigma(E + V \times B) - \frac{\omega_e \tau_e}{B_0}(J \times B) + \frac{\omega_e \tau_e \beta_i}{B_0^2}((J \times B) \times B) \quad (11)$$

Further assumption $\omega_e \tau_e \sim O(1)$ and $\omega_e \tau_i \ll 1$, the pressure gradient of electron and effects of thermo-electric are neglected implies E=0 results:

$$(1 + \beta_e \beta_i)J_x + \beta_e J_y = \sigma B_0 v \quad (12)$$

$$(1 + \beta_e \beta_i)J_x + \beta_e J_y = -\sigma B_0 u \quad (13)$$

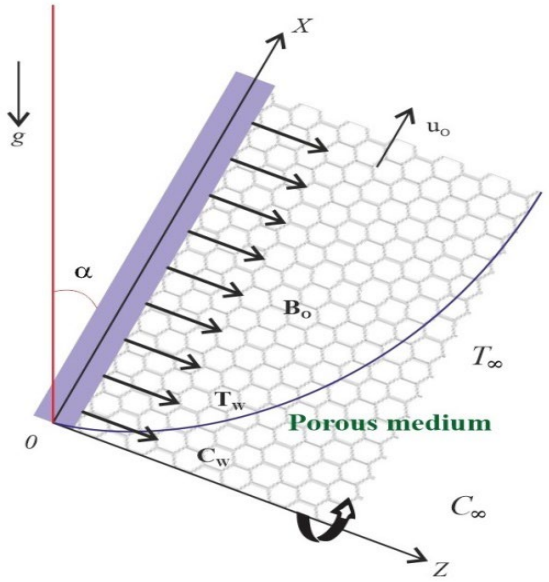

Fig. 1 - Graphical model

By solving Eqs. (12) and (13) we get:

$$J_x = \sigma B_0\left(\frac{\beta_e}{(1+\beta_e\beta_i)^2+{\beta_e}^2}u + \frac{1+\beta_e\beta_i}{(1+\beta_e\beta_i)^2+{\beta_e}^2}v\right) \quad (14)$$

$$J_y = -\sigma B_0\left(\frac{\beta_e}{(1+\beta_e\beta_i)^2+{\beta_e}^2}v - \frac{1+\beta_e\beta_i}{(1+\beta_e\beta_i)^2+{\beta_e}^2}u\right) \quad (15)$$

By non-dimensional terms:

$u' = uu_0$,$v' = vu_0$, $t' = \frac{tv}{u_0^2}$, $z' = \frac{zv}{u_0}$,$a' = \frac{au_0^2}{v}$, $\theta = \frac{T-T_\infty}{T_\omega - T_\infty}$, $\phi = \frac{C-C_\infty}{C_\omega - C_\infty}$, $Gr = \frac{g\beta v(T_\omega - T_\infty)}{u_0^3}$

$Pr = \frac{\mu C_p}{k_1}$, $Gm = \frac{g\beta^* v(C_\omega - C_\infty)}{u_0^3}$, $M = \frac{\sigma B_0^2 v}{\rho u_0^2}$, $K = \frac{ku_0^2}{v^2}$, $Kr = \frac{vKr^*}{u_0^2}$, $Ra = \frac{16a^* v^2 \sigma T_\infty}{k_1 u_0^2}$, $S = \frac{S^* v}{\rho C_p u_0^2}$ $Sc = \frac{v}{D}$,

$R = \frac{2\Omega v}{u_0^2}$, $Ec = \frac{u_0^2}{\rho C_{p(T_\omega - T_\infty)}}$

Hence the governing equations reduces to:

$$\frac{\partial^2 u}{\partial z^2} - \frac{\partial u}{\partial t} = -Gr\theta\cos\alpha - Gm\phi\cos\alpha - \left(\frac{M^2(1+\beta_e\beta_i)}{(1+\beta_e\beta_i)^2+{\beta_e}^2} - \frac{1}{K}\right)u - \left(\frac{M^2\beta_e}{(1+\beta_e\beta_i)^2+{\beta_e}^2} - R\right)v \quad (16)$$

$$\frac{\partial^2 v}{\partial z^2} - \frac{\partial v}{\partial t} = \left(\frac{M^2(1+\beta_e\beta_i)}{(1+\beta_e\beta_i)^2+{\beta_e}^2} + \frac{1}{K}\right)v + \left(\frac{M^2\beta_e}{(1+\beta_e\beta_i)^2+{\beta_e}^2} + R\right)u \quad (17)$$

$$\frac{\partial^2 \theta}{\partial z^2} - Pr\frac{\partial \theta}{\partial t} = (SPr + Ra)\theta - PrEc\left(\frac{\partial u}{\partial z}\right)^2 \quad (18)$$

$$\frac{\partial^2 \phi}{\partial z^2} - Sc\frac{\partial \phi}{\partial t} = ScKr\phi \quad (19)$$

The above equations have initial and boundary conditions as:

$u = v = 0 \quad , \qquad \theta = 0 \quad , \phi = 0 \quad , \forall z \quad , \mathrm{t} \qquad \leq 0$ (20)

$u = e^{at}, \theta = t \, , \phi = t \quad \text{at} \quad z = 0 \, .$ (21)

$u \to 0, \quad \phi \to 0 \, , \theta \to 0 \, , \quad \text{as} \qquad z \to \infty .$ (22)

3. Solution of The Problem

Equations (16), (17), (18), (19) nonlinear equation and their boundary conditions (20), (21), (22) are numerically solved for concentration, temperature, and velocity distributions. The procedure is discussed by Bathe (28) and Reddy (29). The FEM is applied to get accurate and reliable solutions for coupled nonlinear equation and their boundary conditions. The fundamental steps are Domain Elements Discretization; the elements of domain are separated into finite count of sub intervals which is termed as discretization. Every sub interval is now a finite count. The group of these sub intervals is termed as limited mesh. The finite element equations derivation of consists of three steps, Construction of variation formulation for differential equation, Assumption of approximate solution for characteristic finite element. Derivation of finite element equation is obtained by substituting the solution in variation formulation, Element equation assembly. The results obtained by the above procedure are assembled by subjecting to inter-element continuity conditions. These results to many algebraic equations making into global finite element model governing whole flow domain. The boundary conditions of equations (20), (21), (22) are applied for these assembled equations. The final set of equations is solved directly or by iterative numerical methods. Numerical solutions of these equations were obtained by MATLAB. By changing the values of velocity, temperature, and concentration the stability and convergence of finite element method was tested. The results were more than satisfactory.

4. Results and Discussion

The illustrative interpretation of mass and heat transfer flows represents the nature of various parameters which govern the flow. Figures 2-5 represent velocities; Illustration 6 represent temperatures; Figure 7 represent concentrations profiles and Figure 8 represent secondary velocity. The results validation is done in Table which illustrates viscous dissipation Ec. When a=0 the plate is at constant motion. For a>0 temperature, velocity and concentration induces higher starting value. For the profiles various values are fixed t=0.5 and the various parameters are Gr =3, Gm=2, M=0.5, K=1, Kr =1, Sc=0.22, Pr =0.71, a=0.2, $\alpha=\pi/6$, S=1, β_e=0.2, Ra=2, β_i=1, S=1, R=0.5. Figure 2 (a) represents the velocity profiles for M Hartmann number, velocity decreases because of magnetic field. Drag force known as Lorentz decreases velocity in the fluid region, hence unnoticed decrement in speed is noticed in area by relevance of magnetic field. It is also noticed that magnetic field trims down velocity distribution on all sides thus retarding effect is observed on velocity profile and thick momentum boundary layer is formed. Figure 2 (b) represents the velocity profiles for Permeability number, from this figure as K increases the velocity also grows and then eventually widens the width of the momentum boundary layer. If the ability to penetrate of the porous medium is less than if K is less, then it results in velocity to decrease in flow field and it impacts the thickness of momentum boundary layer.

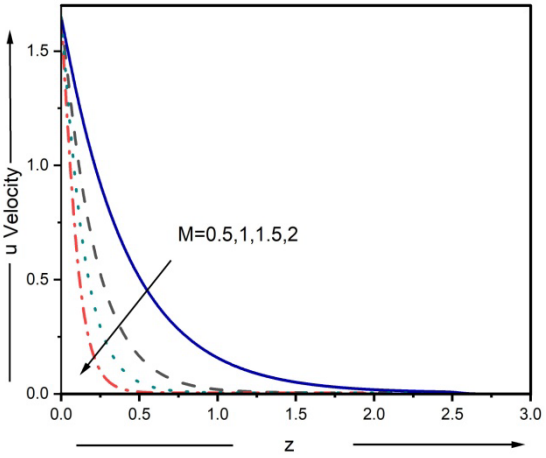

Fig. 2(a) - Profile of velocity for different values for M

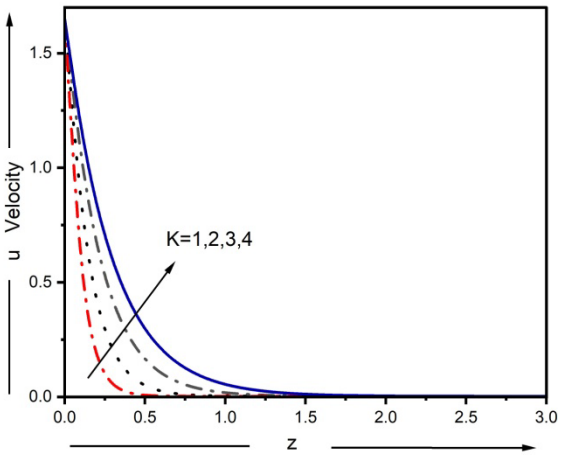

Fig. 2(b) - Profile for velocity for different values of K

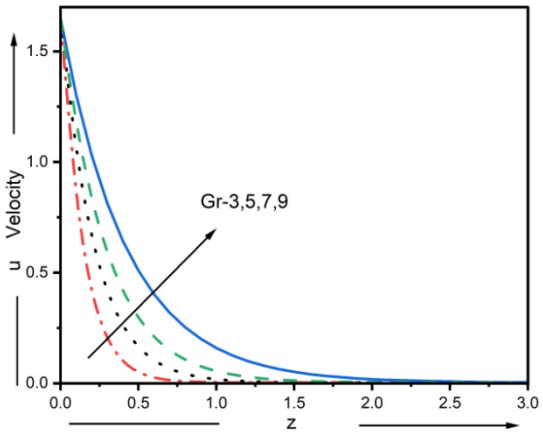

Fig. 2(c) - Profile of velocity for different values of Gr

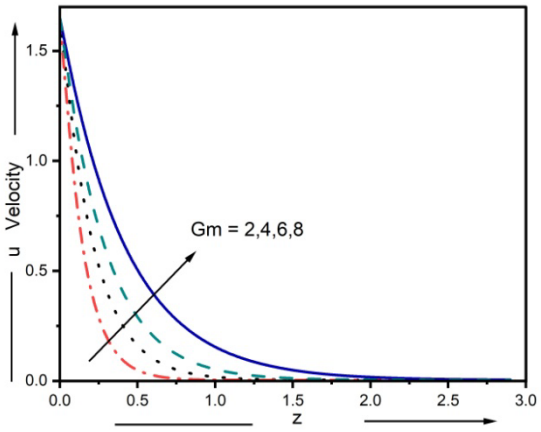

Fig. 2(d) - Profile of velocity for different values of Gm

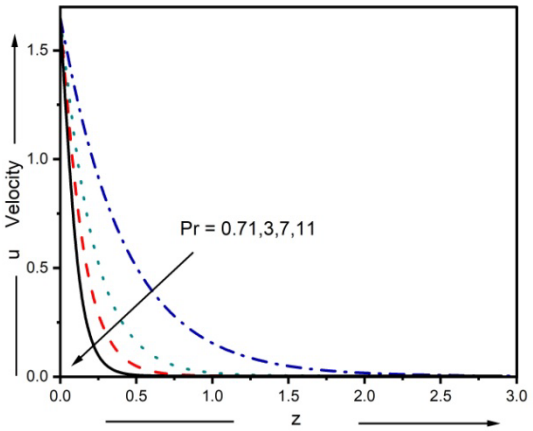

Fig. 3(a) - Profile of velocity for different values of Pr

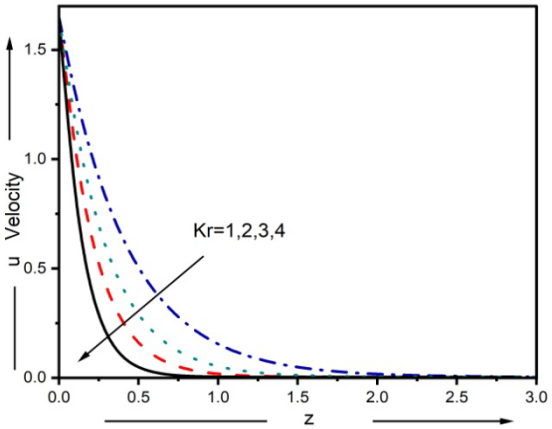

Fig. 3(b) - Profile of velocity for different values of Kr

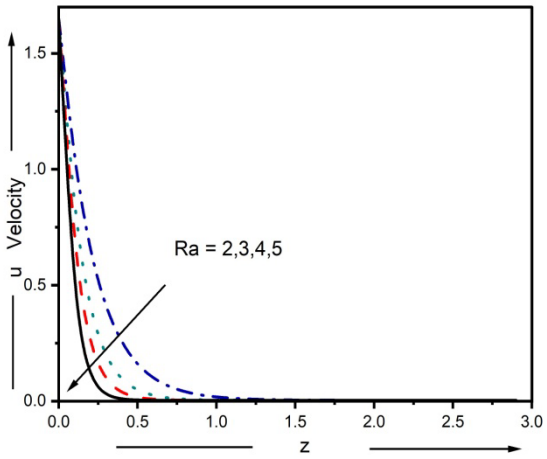

Fig. 3(c) - Profile of velocity for different values of Ra

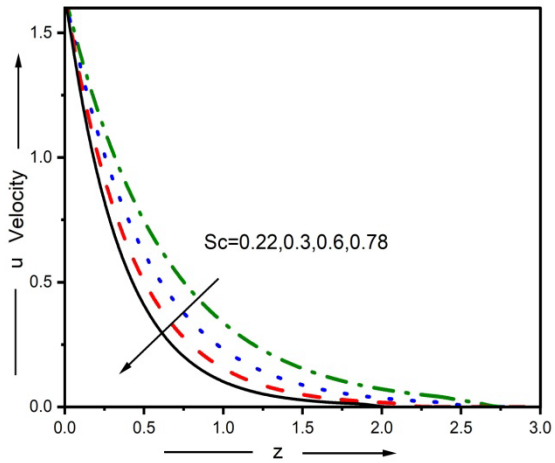

Fig. 3(d) - Profile of velocity for different values of Sc

Figure 2 (c) represents the velocity profiles for Gr Grashof number, increase in Gr increases velocity and thickness of boundary layer. Gr specifies thermal forces of buoyancy to that of hydrodynamic viscous forces. Increase in buoyancy forces means increase in wall temperature hence the bond between internal friction decreases and gravity is stronger, so velocity increases Figure 2 (d) represents the velocity profiles for Gm mass Grashof number exhibits effects of Gm on resultant fluid velocity. There is an increase in velocity of fluid flow with increase in Gm. It is observed that velocity of fluids increases with strengthening of solute buoyancy and heat forces, the velocity distribution increases sharply immediately beside to porous surface and later there is decay to initial velocity and

reaches to zero smoothly. This reason causes thickness of momentum boundary layer to increase. Hence velocity increases with increase in Gm.

Figure 3 (a) represents the velocity profiles for Prandtl number Pr, we noticed that increase in Pr decreases velocity in fluid flow therefore momentum boundary layer tends to diminish with increment in Pr. Increase in Pr makes fluid movement decrease resultant velocity. Highest Prandtl number has high viscosity which makes fluid have substantial thickness. Hence the velocity profile decreases. Figure 3 (b) represents the velocity profiles for Kr Chemical reaction parameter, we noticed that increment in Kr decreases slightly velocity in fluid flow. Chemical reaction parameter Kr increase suppress concentration of fluid and molecular diffusivity lessens due to increase in Kr. This results in velocity reducing slightly. Figure 3 (c) represents the velocity profiles for radiation parameter Ra, we noticed that as there is variation in Ra that is increase in Ra decreases velocity in fluid flow. It is also observed that there is decrease in velocity of fluid flow inside boundary layer due to increase in thermal radiation parameter. Further it is observed that spike in velocity of fluid boosts nearby surfaces to grow mouldl approaching to zero. As conclusion it is evident that thickness of momentum boundary layer increases with increase in heat radiation parameter. Figure 3(d) represents the velocity profiles for Schmidt number Sc, we noticed that increment in Schmidt number increases chemical reaction rate which leads to reduction of velocity. Also noticed that increase in Schmidt number results in reduction of thickness of momentum boundary layer. Hence there is a decrease in velocity profile with increase in Sc.

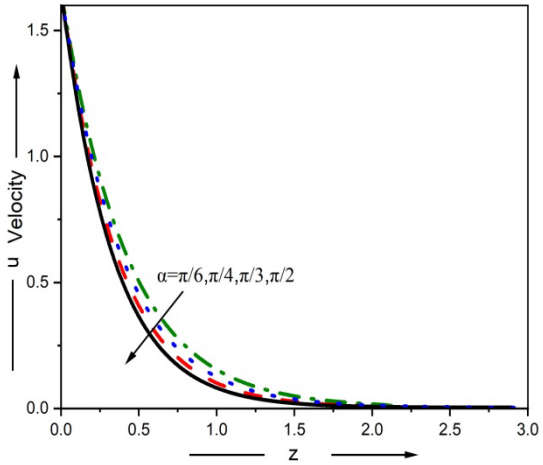

Fig. 4(a) - Profile of velocity for different values of α

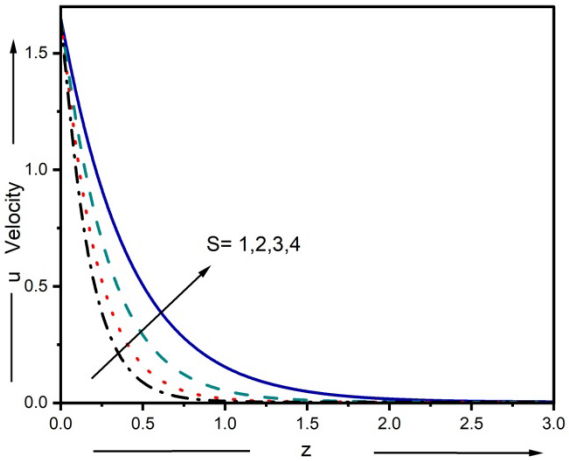

Fig. 4(b) - Profile of velocity for different values of S

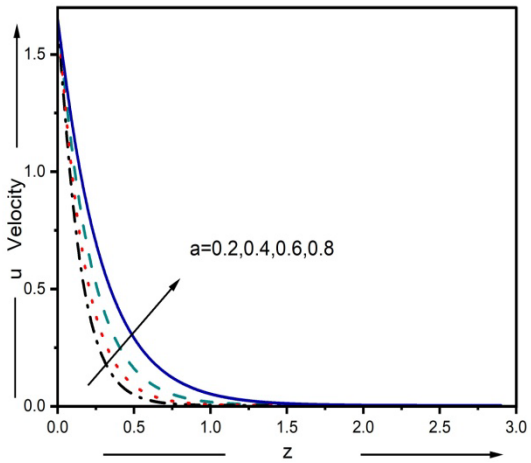

Fig. 4(c) - Profile of velocity for different values of a

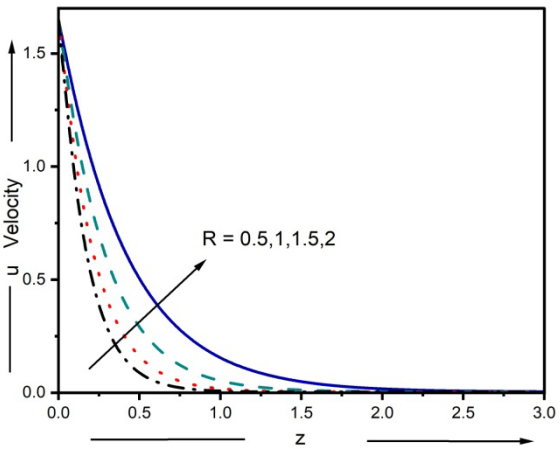

Fig. 4(d) - Profile of velocity for different values of R

Figure 4 (a) represents the velocity profiles for inclined angle of the plate, we noticed that increase in inclined angle tends to reduce velocity because cosine of α depletes forces influencing velocity's increase. Hence velocity profile decreases with increase in inclination of angle of the plate. Figure 4 (b) represents the velocity profiles for S heat source parameter increase due constant rotation which in turn increases velocity. Further observed that heat source parameter positively affects velocity of fluid flow. Heat source parameter increases thickness momentum boundary layer to increase hence it develops spike in fluid velocity next to the plate. Figure 4 (c) represents the velocity profiles for acceleration parameter has a positive effect on velocity profile. The increase in acceleration in flow field increases the movement of fluid hence by natural convection as acceleration increases velocity of fluid increases. Figure 4 (d)

represents the velocity profiles for R rotation parameter increases velocity with its increase. This parameter increases the fluid velocity throughout the flow. The effect of acceleration is large near the axis or rotation due to Coriolis force. Hence momentum boundary layer thickness increases with increase in rotation. This results in increases of velocity. Figure 4(4) represents the velocity profiles for Ec Eckert number decreases velocity with its rise. The fluid velocity for different values of Ec shows that increase in Ec develops a drop in fluid velocity next to the plate. The thickness of velocity boundary layer will be minimum at plate for velocity profile attaining its minimum value. Figure 5 (a) represents the velocity profiles for Hall parameter β_e increases velocity with its increase. Magnetic resistive force is dropped by conductivity which results in an increase in velocity. The Hall parameter β_e decreases magnetic fierceness and increases conductibility which in turn spikes velocity. As a result, velocity increases. Figure 5 (b) represents the velocity profiles for Ion slip parameter β_i also increases velocity with it increase. Damping forces decrease with increase in conductivity which is due to increase in β_i. This effect causes high conductivity and results in spike of velocity.

Figure 6 (a) represents the velocity profiles for Pr Prandtl number decreases thermal diffusivity with increase in its value. Increase in Pr makes fluid movement decrease and thermal temperature. The highest Prandtl number has high viscosity which makes fluid have substantial thickness in energy boundary layer. Hence the temperature decreases. Figure 6 (b) represents the velocity profiles for S Heat source parameter decreases temperature profile. Thermal boundary layer thickness reduces with rise in S heat source parameter. Hence temperature profile decreases. Figure 6 (c) represents the velocity profiles for Ra radiation parameter decreases temperature with its increase. It is observed that temperature in the boundary layer decreases with increase in thermal radiation parameter. It is because, increase in Ra results in increase of heat radiation in the thermal boundary layer which consequently decreases temperature profile in thermal boundary layer. Figure 6 (d) represents the velocity profiles for T elapse in time results in higher temperature. A temperature profile is a complex time temperature data and related to measuring temperature in an oven. The temperature profile is measured along slope. Hence time elapses in fluid flow increases temperature profile. Figure 6 (e) represents the velocity profiles for Ec Eckert number increases temperature profile. It is noticed that temperature profile is maximum at plate and increase exponentially and fall to zero away from the plate. The thickness of the thermal boundary layer increases comparatively with increase in Ec, hence temperature profile increases with increase in Ec.

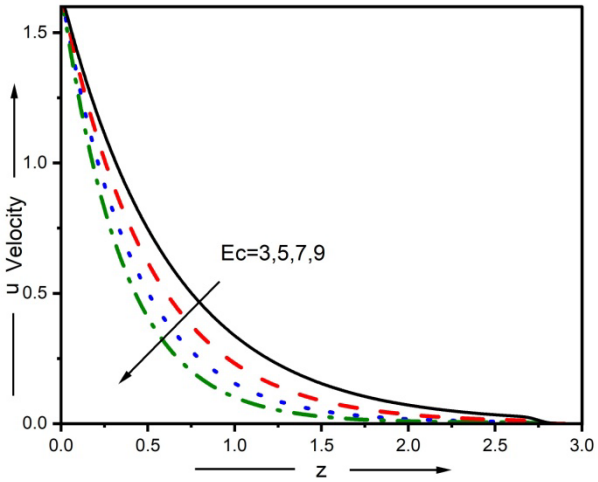

Fig. 4(e) - Profile of velocity for different values of Ec

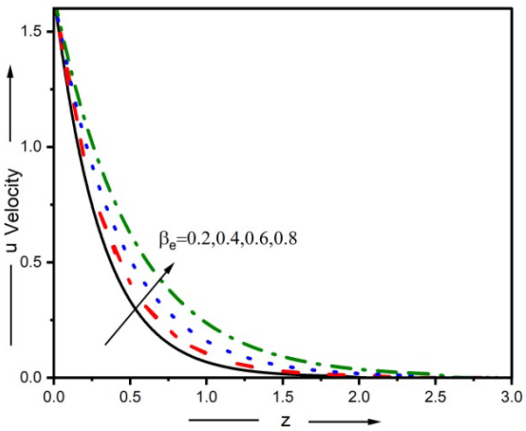

Fig. 5(a) - Profile of velocity for different values of β_e

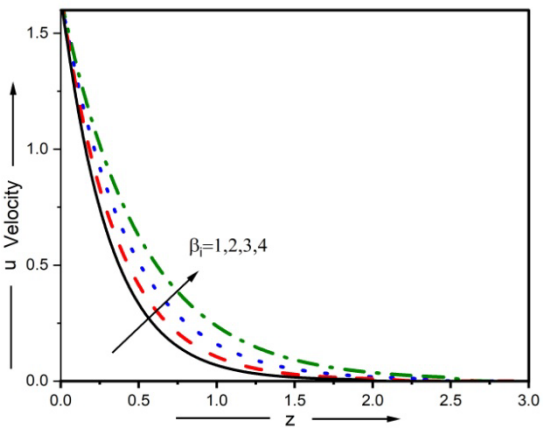

Fig. 5(b) - Profile of velocity for different values of β_i

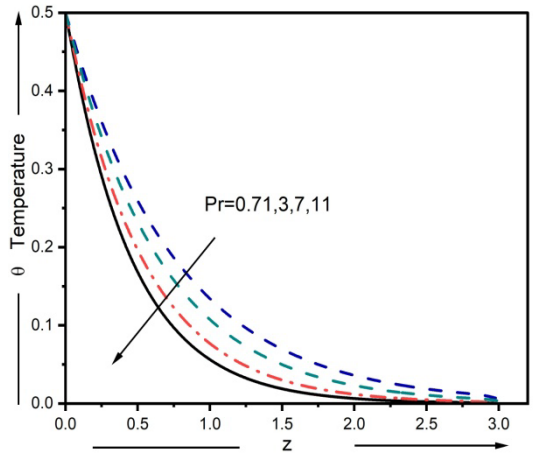

Fig. 6(a) - Profile of temperature for different values of Pr

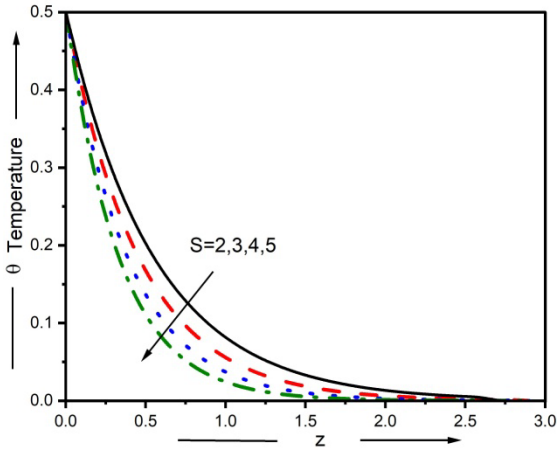

Fig. 6(b) - Profile of Temperature for different values of S

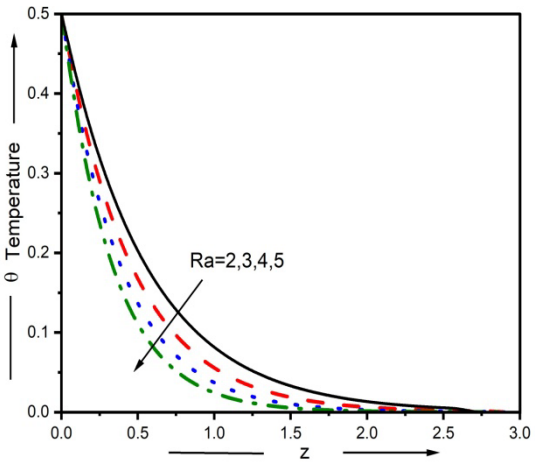

Fig. 6(c) - Profile of Temperature for different values of R

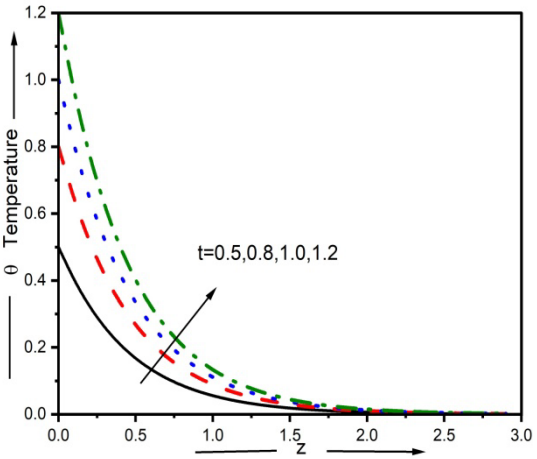

Fig. 6(d) - Profile of Temperature for different values of t

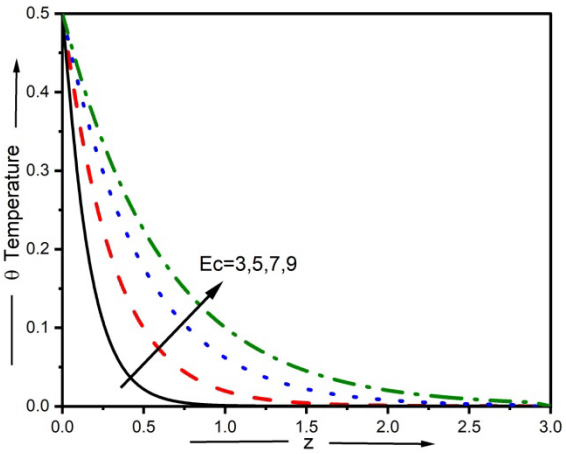

Fig. 6(e) - Profile for Temperature for different values of Ec.

Figure 7 (a) represents the velocity profiles for Kr, parameter of chemical reaction increase tends to diminish concentration profile drastically. The reason being increase in number of molecules in chemical reaction parameter increases and results in concentration decrease. Figure 7(b) represents the velocity profiles for Sc Schmidt number increase results in weaker solute diffusivity which results in decrease of concentration. It is observed that concentration of fluid is maximum on surface of plate then decreases and disappears away from the plate. Sc Schmidt number higher values means higher bread which results in lesser diffusion and lessening of concentration in fluid region. Hence concentration boundary layer thickness decreases by increase in Sc. Figure 7 (c) represents the velocity profiles for t

increase of time increases concentration in fluid region. It is observed that the rate of reaction changes in concentration dependent on time. As the reaction progresses the change in concentration of reactants decreases and the concentration profile increases with time. Figure 8 (a) represents the velocity profiles for M Hartmann number, secondary velocity decreases because of magnetic field. Drag force known as Lorentz decreases secondary velocity in the fluid region, hence unnoticed decrement in speed is noticed in area by relevance of magnetic field. It is also noticed that magnetic field trims down secondary velocity distribution on all sides thus retarding effect is observed on velocity profile and thick momentum boundary layer is formed. Figure 8 (b) represents the velocity profiles for K. Permeability number, from the figure, it is evident that as K grows the secondary velocity also increases and hence thickness of momentum boundary layer follows. From the figure as K increases the secondary velocity also grows and then eventually widens the width of the momentum boundary layer. If the ability to penetrate of the porous medium is less than if K is less then it results in secondary velocity to decrease in flow field, and it impacts the thickness of momentum boundary layer. Figure 8 (c) represents the velocity profiles for R rotation parameter increases secondary velocity with its increase. This parameter increases the fluid velocity throughout the flow.

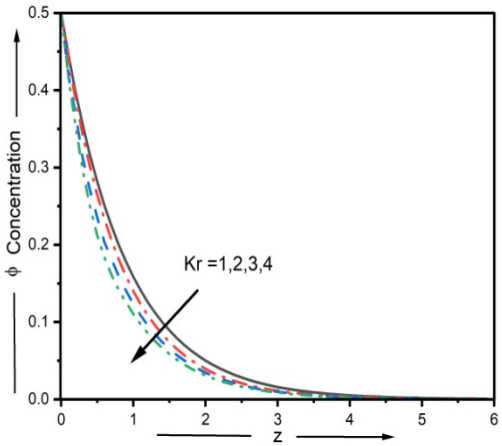

Fig. 7(a) - Profile of concentration for different values of Kr

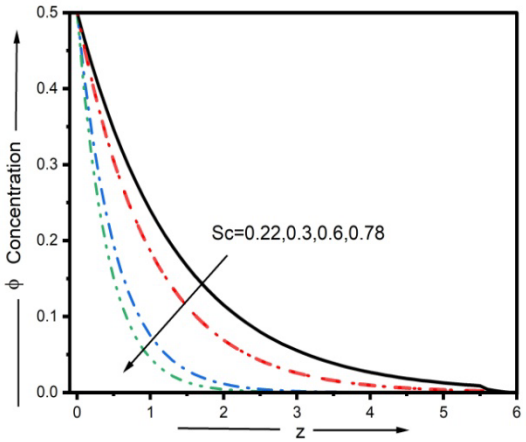

Fig. 7(b) - Profile of concentration for different values of Sc

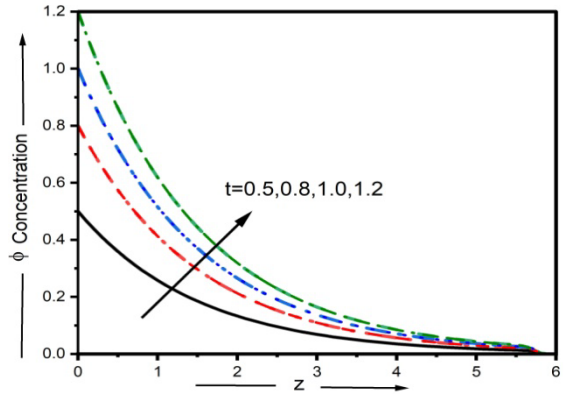

Fig. 7(c) - Profile of concentration for different values of t

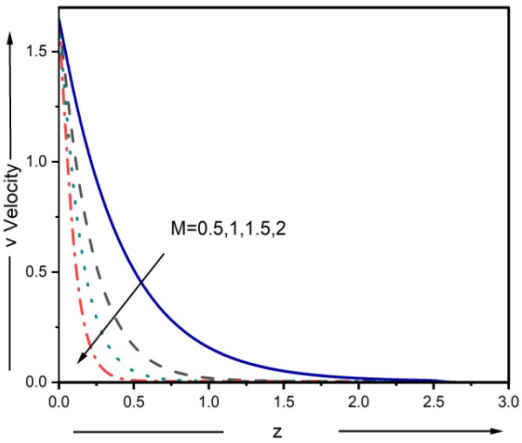

Fig. 8(a) - Profile of velocity for different values for M

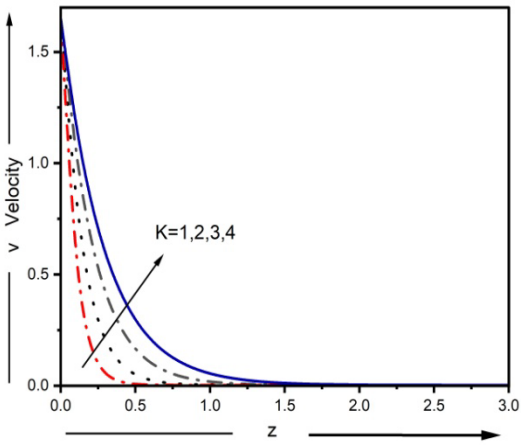

Fig. 8(b) - Profile for velocity for different values of K

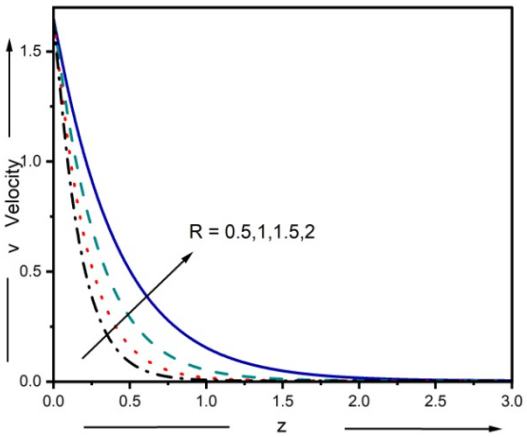

Fig. 8(c) - Profile of velocity for different values of R

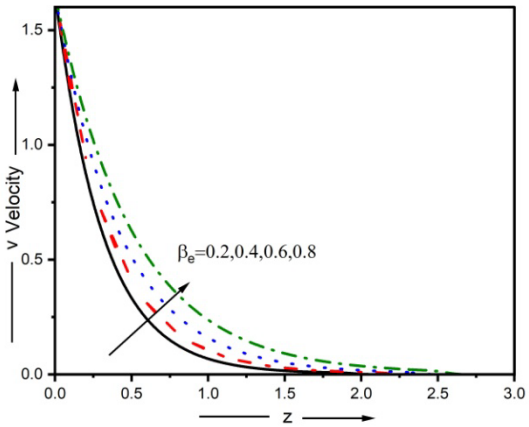

Fig. 8(d) - Profile of velocity for different values of be β_e

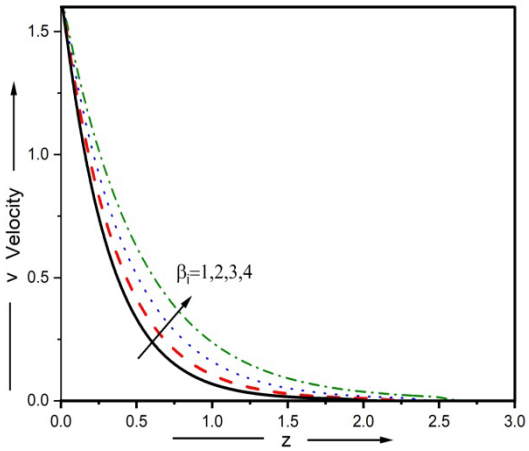

Fig. 8(e) - Profile of velocity for different values of β_i

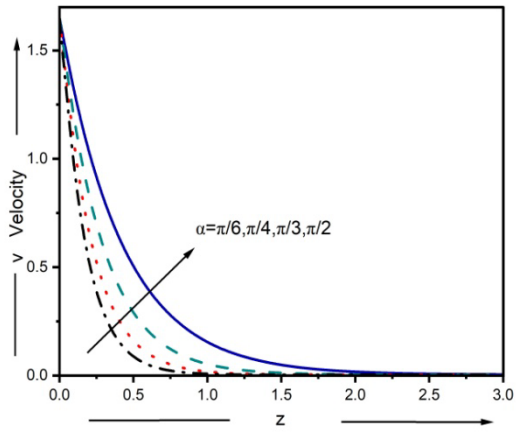

Fig. 8(f) - Profile of velocity for different values of α

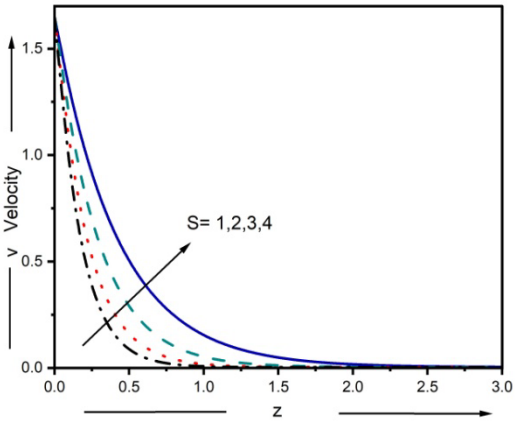

Fig. 8(g) - Profile of velocity for different values of S

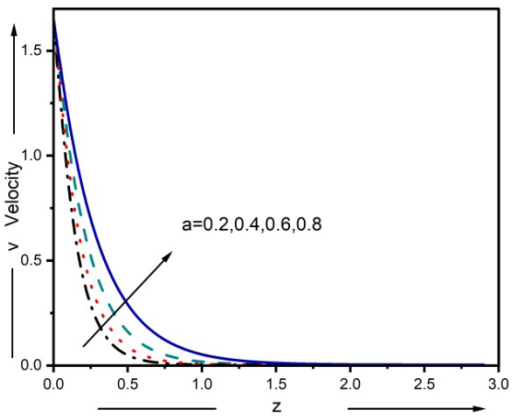

Fig. 8(h) - Profile of velocity for different values of a

The effect of acceleration is large near the axis or rotation due to coriolis force. Hence momentum boundary layer thickness increases with increase in rotation. This results in increases of secondary velocity. Figure 8 (d) represents the velocity profiles for Hall parameter β_e increases secondary velocity with its increase. Magnetic resistive force is dropped by conductivity which is result of increase in β_e. Figure 8 (e) represents the velocity profiles for Ion slip parameter β_i also increases secondary velocity with it increase. Damping forces decreases with increase in conductivity which is due to increase in β_i Figure 8 (f) represents the velocity profiles for α inclined angle of the plate, we noticed that increase in inclined angle tend to reduce secondary velocity because cosine of α depletes forces influencing velocity. α inclined angle of the plate, we noticed that increase in inclined angle tend to reduce secondary velocity because cosine of α depletes forces influencing velocity's increase. Hence secondary velocity profile decreases with increase in inclination of angle of the plate. Figure 8 (g) represents the velocity profiles for S heat source parameter increase due constant rotation which in turn increases secondary velocity S heat source parameter increase due constant rotation which in turn increases secondary velocity. Further observed that heat source parameter positively affects velocity of fluid flow. The heat source parameter increases thickness momentum boundary layer to increase hence it develops spike in fluid's secondary velocity next to the plate. Figure 8 (h) represents the velocity profiles for an acceleration parameter that has a positive effect on velocity profile. The increase in acceleration in flow field increases the movement of fluid hence by natural convection as acceleration increases secondary velocity of fluid increases.

5. Validation of Numerical Results

We compared the current results to confirm the genuineness of the numerical results obtained by applying MATLAB code. In the absence of viscous dissipation Ec=0, the effects of M, K, S, Ra on skin friction coefficient and earlier published numerical results are compared in Table below. It agrees that present numerical results are very close to the results stated by Pattnaik et al. [30] and Krishna et al. [31] as shown in Table. Therefore, the developed code has confidence in the numerical results studied in this article.

Table 1 - Comparison of velocity component (u) when viscous dissipation Ec=0.

M	K	S	Ra	Pattnaik et al. [30]	Veera Krishna et al. [31]	Present Results
0.5	1.0	1.0	2.0	0.671987	0.671989	0.671988
1.0	1.0	1.0	2.0	0.610769	0.610770	0.610770
1.5	1.0	1.0	2.0	0.527190	0.527191	0.527190
0.5	2.0	1.0	2.0	0.668627	0.668626	0.668627
0.5	3.0	1.0	2.0	0.579948	0.579947	0.579949
0.5	1.0	2.0	2.0	0.676540	0.676539	0.676541
0.5	1.0	3.0	2.0	0.681819	0.681820	0.681820
0.5	1.0	1.0	3.0	0.666571	0.666570	0.666570
0.5	1.0	1.0	4.0	0.662057	0.662058	0.662058

6. Conclusion

We analyzed the MHD fluids for ion slip and Hall effects on free unsteady convective flow for inclined accelerated exponential plate for saturated permeable medium. In analysis we considered the effect of variable temperature, the angle of inclination along with concentration. The results observed are:

a. Effects of ion slip and Hall presence increases velocity profile both primary and secondary and prevents front flow of fluid.
b. Chemical reactions, angle of inclination and fluid being heavy with species resist velocity.
c. Rotation, Hall, and ion slip effect speeds up the motion of fluid.
d. Radiation parameter decreases velocity, decreases temperature there by reaching stable state.
e. Concentration levels diminish with an increase in chemical reaction rate.

Acknowledgements

Pratapa Kamala sincerely acknowledges support of Corresponding author and support by Department of Mathematics GITAM University, Hyderabad, India.

References

[1] M.Veera Krishna, "Thermo diffusion, chemical reaction, and Hall and ion-slip impacts on MHD rotating flow past an infinite vertical porous plate". wileyonlinelibrary.com/journal/htj Heat Transfer, 1-27, (2021).
[2] Mukhopadhyay S, 'The effects of thermal radiation on unsteady mixed convection flow and heat transfer over a porous stretching surface in porous medium'. Int J Heat Mass Transfer, 52, 3261-3265, (2009).
[3] P.C.Ram, "The effects of Hall and ion slip currents on free convective heat generating flow in a rotating fluid", Int.J.Energy Res, 19(5), 371-376, (1995).
[4] M.A. Seddeek, "The Effects of Hall and ion –Slip currents on magneto-micro polar fluid and heat transfer over a non-isothermal stretching sheet with suction and blowing", Proc, Royal Soc.: Lond. A, 457, 3039-3050, (2001).
[5] M.M.Bhatti, "M.A. Abbas. M.M.Rashidi. Effect of Hall and ion slip on Peristaltic blood flow of Eyring Powell fluid in a non-uniform permeable channel", World J.Modell.Simul, 12(4), 268-279, (2016).
[6] Z. Uddin, M.Kumar , "Hall and ion slip effect on MHD boundary layer flow of a micro polar fluid past a wedge", Scientia Iranica B, 20 (3), 467-476, (2013).
[7] K.S Jitendra, C.T. Srinivasa, "Unsteady natural convection flow of a rotating fluid past an exponential accelerated vertical plate with Hall current, ion-slip and magnetic effect, Multidisc. Model". Mater. Struct. 13(2), 216-235, (2018).
[8] M.Veera Krishna, A.J.Chamkha, "Hall effects on MHD Squeezing flow of a water based nano fluid betweentwo parallel disks", J.Porous Media, 22(2), 209-223, (2019).
[9] M.Veera Krishna, Ali J.Chamkha, "Hall and ion slip effects on MHD rotating boundary layer flow of Nano fluid past an infinite vertical plate embedded in a porous medium", Results Phys, 15, 102652, (2019).
[10] M.Veera Krishna, B.V. Swarnalathamma, A.J.Chamkha, "Investigations of Soret,Joule and Hall effectson MHD rotating mixed convective flow past an infinite vertical porous plate", J.Ocean Engg. Sci., 4(3), 263-275, (2019).
[11] A.T. Mohamed, F.E. Ahmed, Z.M. Enass, "Numerical simulation of double-diffusive natural convective flow in an inclined rectangular enclosure in the presence of magnetic field and heat source", Int.J.Therm.Sci.,52(1), 161-175, (2012).
[12] Khilap Singhm, Alok kumar Pandey, Manoj kumar, "Analytical approach to stagnation-point flow and heat transfer of a micro polar fluid via a permeable shrinking sheet with slip and convective boundary conditions,,Heat Transf". Res., 59 (8), 739-756, (2019).
[13] Padam Singh, Alok kumar Pandey, Manoj kumar , "Forced convection in MHD slip flow of alumina waterNano fluid over plate", J.Enchanced Heat Transf., 23 (6), 487-497, (2016).
[14] Alok kumar Pandey, Manoj Kumar, "Effect of viscous dissipation and suction/injection on MHD Nanofluid flow over a wedge with porous medium and slip", Alex Engg.J., 55 (4), 3115-3123, (2016).
[15] Alok Kumar Pandey, Manoj Kumar, "Natural convection and thermal radiation influence on Nanofluid flow over a stretching cylinder in a porous medium with viscous dissipation", Alexandria Eng.J., 56 (1), 55-62, (2017).
[16] Malvandi A, Hedayati F and Ganji, "DD Slip effects on unsteady stagnation point flow of a Nano fluid over a stretching sheet", Powder Technology, 253, 377-384, (2014).
[17] Satya Narayana PV, Venkteswarulu B and venkataramana.S, "Effects of Hall current and radiation absorption on MHD micro polar fluid in a rotating system", Ain Shams Engineering Journal, 4(4), 843-854, (2013).
[18] Sugunamma V, Sandeep N. Mohan P.K. and Ramana B. "Inclined Magnetic field and Chemical ReactionEffects on flow over a Semi Infinite vertical porous plate through porous medium communication",in Applied Sciences ISSN 2201-7372, 1, 1-24, (2013).
[19] Amos E and Omamoke E.MHD, "Free Convective Flow over an Inclined porous surface with variablesuction and Radiation Effects". International Journal of Applied Science and Mathematical Theory, ISSN, 2489-009X, 4(3), (2018).

[20] Mutuku-Njane WN, Makinde OD. "On hydro magnetic boundary layer flow of nano fluids over a permeable moving surface with Newtonian heating", Latin Am Appl Res 44, 57-62, (2014).
[21] Hamad MAA, Pop I. "Unsteady MHD free convection flow past vertical permeable flat plate in arotating frame of reference with constant heat source in a Nano fluid". Heat Mass Transfer, 47, 1517-24, (2011).
[22] Kiran Kumar , RVMSS, Prasad P Durga, Varma SVK. "Thermo diffusion and chemical reaction effects on free convective heat mass transfer flow of conducting Nano fluid through porous medium in a rotating frame". Global J Pure Appl Math, 12, 342-51, (2016).
[23] M.I. Khan, "Transportation of hybrid nanoparticles in forced convective Darcy- Forchheimer flow by a rotating disk, International Communications", in Heat and Mass Transfer, 122, 105177, (2021).
[24] M. Aziz El. Abd and A. A. Afify, "Effect of Hall current on MHD slip flow of Casson Nano fluid over a stretching sheet with zero nanoparticle mass flux", Thermo physics and Aeromechanics, 55(3), 2125-2137, (2016).
[25] S.R. Siva and A.K. Suram and P. Modugulua, "Heat and mass transfer past an impulsively moving vertical plate with ramped temperature", Journal of Applied Science and Engineering, 19 (4), 385-392, (2016).
[26] S.R. Siva and A.K. Suram, "Finite element analysis of heat and mass transfer effects on MHD natural convection flow past an infinite inclined plate with ramped temperature", Journal of the Korean Society for Industrial and Applied Mathematics, 20 (4,) 355-374, (2016).
[27] Bathe, K.J. Finite Element Procedures, Prentice-Hall, New Jersey (1996).
[28] Reddy J N. An Introduction to the Finite Element Method, McGraw-Hill, New York (1985).
[29] J.R. Pattnaik, G.C. Dash, S. Singh, "Radiation and mass transfer effects on MHD flow through porous medium past an exponentially accelerated inclined plate with variable temperature", Ain Shams Engg. J., 8, 67–75, (2017).
[30] M. Veera Krishna, N. Ameer Ahamad, Ali J. Chamkha, "Hall and ion slip effects on unsteady MHD free convective rotating flow through a saturated porous medium over an exponential accelerated plate". Alexandria Engineering Journal, 59, 565-577, (2020).